INL/CON-23-73442-Revision-0

High-fidelity Experiments of Turbulent Buoyant Jets from Simultaneous Particle Image Velocimetry and Laser Induced Fluorescence

August 2023

Valentina Valori, Sunming Qin, Victor Petrov, Annalisa Manera

Changing the World's Energy Future

Idaho National Laboratory

INL is a U.S. Department of Energy National Laboratory operated by Battelle Energy Alliance, LLC

DISCLAIMER

This information was prepared as an account of work sponsored by an agency of the U.S. Government. Neither the U.S. Government nor any agency thereof, nor any of their employees, makes any warranty, expressed or implied, or assumes any legal liability or responsibility for the accuracy, completeness, or usefulness, of any information, apparatus, product, or process disclosed, or represents that its use would not infringe privately owned rights. References herein to any specific commercial product, process, or service by trade name, trade mark, manufacturer, or otherwise, does not necessarily constitute or imply its endorsement, recommendation, or favoring by the U.S. Government or any agency thereof. The views and opinions of authors expressed herein do not necessarily state or reflect those of the U.S. Government or any agency thereof.

INL/CON-23-73442-Revision-0

High-fidelity Experiments of Turbulent Buoyant Jets from Simultaneous Particle Image Velocimetry and Laser Induced Fluorescence

Valentina Valori, Sunming Qin, Victor Petrov, Annalisa Manera

August 2023

Idaho National Laboratory
Idaho Falls, Idaho 83415

http://www.inl.gov

Prepared for the
U.S. Department of Energy
Under DOE Idaho Operations Office
Contract DE-AC07-05ID14517

High-fidelity experiments of turbulent buoyant jets from simultaneous Particle Image Velocimetry and Laser Induced Fluorescence

Valentina Valori[a,b], Sunming Qin[d], Victor Petrov[a,b,c], and Annalisa Manera[a,b,c]
[a]ETH Zürich, Dep. of Mechanical and Process Eng., Nuclear Safety & Multiphase Flows
Sonneggstrasse 3, 8092 Zürich, Switzerland
[b]Paul Scherrer Institute, Laboratory for Reactor Physics and Thermal-Hydraulics
Forschungsstrasse 111, 5232 Villigen PSI, Switzerland
[c]University of Michigan, Department of Nuclear Engineering & Radiological Sciences
2355 Bonisteel Boulevard, Ann Arbor, Michigan 48105
[d]Idaho National Laboratory, 1955 N. Fremont Ave. Idaho Falls, ID 83415
vvalori@ethz.ch; sunming.qin@inl.gov; vpetrov@ethz.ch; maneraa@ethz.ch

ABSTRACT

Accurate models of turbulent buoyant flows are essential for the design of nuclear reactors thermal hydraulics and passive safety systems. However, available models fail to fully capture the physics of turbulent mixing when buoyancy becomes predominant with respect to momentum. Therefore, high-fidelity experiments of well-controlled fundamental flows are needed to develop and validate more accurate models. We performed experiments of positive and negative turbulent buoyant jets, both in uniform and stratified environments, with the aim of understanding the thermal hydraulics of turbulent mixing with variable density and providing high-fidelity data for the development and validation of turbulence models. Non-intrusive, simultaneous Particle Image Velocimetry and Laser Induced Fluorescence measurements were carried out to acquire instantaneous velocity and concentration fields on a vertical section parallel to the axis of a jet in the self-similar region. The Refractive Index Matching method was applied to measure high-resolution buoyant jets with up to 8.6% density difference. These data are free of the typical errors that characterize optical measurements of buoyancy driven flows (e.g., natural and mixed convection) where the refractive index of the fluid is inhomogeneous throughout the measurement domain. Turbulent statistics and entrainment of buoyant jets in uniform and stratified environments are presented. These data are compared with non-buoyant jets in uniform environment, as a reference to investigate the effects of buoyancy and stratification on turbulent mixing. The results will be used for the assessment of current turbulence models and as basis for the development of a new one that captures turbulent mixing.

KEYWORDS

Turbulent buoyant jets, Refractive Index Matching, PIV, LIF, Turbulent mixing.

1. INTRODUCTION

Turbulent buoyant jets in density stratified environments have many geophysical and technological applications, such as volcanic eruptions and emissions from industrial chimneys. Density effects like fluid stratification play a significant role in nuclear power plants [1], especially in the design of safety systems.

In a typical light water reactor, it is crucial to understand and predict the complicated thermal-hydraulics phenomena, which occurs in the containment atmosphere in case of severe accidents. As the Three Mile Island accident in 1979 and the Fukushima Daiichi nuclear disaster in 2011 have shown, overheating in the reactor core caused a reaction between the water and the zircaloy to create hydrogen gases, which is a serious threat since the mixture of hydrogen and oxygen is highly flammable an explosive. Due to its light weight, hydrogen will float and accumulate in the upper plenum of the containment, forming a stratification region. By investigating the heat and mass transfer in buoyancy driven flows, as Deri et. al. [2] mentioned in their study, features can be designed to break the stratification in the containment building, such as sprays injection and gas jets. In addition, thermal mixing and stratification phenomena with liquid fluid in large pools play an important role for safety and operation of several Gen-IV reactor systems, like for example, in the temperature distribution in the cold and hot pool of sodium-cooled fast reactors [3].

When a fluid is injected in an environment with different density, both momentum and buoyancy forces contribute to its motion. If the environment is lighter than the injected fluid, as for positive buoyant jets, the two forces act in the same direction. When the environment is heavier, as for negative buoyant jets, buoyancy acts in the opposite direction with respect to momentum. Both positive and negative buoyant jets have been investigated experimentally and theoretically for homogenous and linearly stratified environments in the works of Abraham [4], Turner [5], Fischer et. al. [6], List [7], and Bloomfield & Kerr [8, 9]. These studies were mainly based on qualitative measurement techniques using color dye, to estimate the width of the buoyant jet and the jet final heights (penetration depths). When a fluid is injected in a two-layer stratified environment with heavier fluid at the bottom (see for example Figure 1, right panel), the momentum force is enhanced by the effect of buoyancy in the bottom layer, while it is contrasted in the top one. If the momentum is not large enough, the jet may behave like a fountain and reverse its direction at the interface. For the buoyant jet interacting with a two-layer stratified environment, Lin and Linden [10] studied the entrainment of a turbulent fountain at a steady density interface. Mott and Woods [11] investigated and developed a model to describe the mixing of two-layer and linear stratifications with turbulent positively buoyant plumes. Deri et. al. [2] created a stratified environment using air and helium and analyzed the mixing characteristics across the stratification layers. All these studies were performed using gaseous flows with large Reynolds numbers. Fewer studies have been carried out with liquid flows instead. Shy [12] investigated the mixing processes involving organized large-scale motion and chaotic small-scale motions across a sharp density interface experimentally via a pH-sensitive, laser-induced fluorescence technique in a water tank. Ansong et al. [13] studied the penetration depth of a water fountain (dyed with food coloring) impinging on a density interface. Shakouchi et al. [14] used water and a NaCl-water solution to create a density interface and visualized the jet impacting into two-layer density interface. After conducting an extensive review of the turbulent mixing in stratified flows, Fernando [15] concluded that there is still a lack of consensus in the characterization of the mixing behavior.

Due to the limitation of the current computational power, turbulence modeling is indispensable since resolving the whole range of spatial and temporal scales of the real-world turbulent problems with direct numerical simulations is impossible. Most of the CFD simulations performed nowadays are based on space filtering when large eddy simulations (LESs) are used and time filtering for the use of Reynolds-Averaged Navier-Stokes (RANS) model. According to the statistical approaches, RANS model decomposes the time-dependent variables of the NS equations into a time-averaged quantity with a fluctuating one; for example, the instantaneous velocity $\boldsymbol{u}_j = \overline{u_j} + u_j'$. With Einstein notations, the governing equations that describe the fluid motion will have the following form:

$$\frac{\partial \rho}{\partial t} + \frac{\partial (\rho \overline{u}_j)}{\partial x_j} = 0, \tag{1}$$

$$\frac{\partial (\rho \overline{u}_i)}{\partial t} + \frac{\partial}{\partial x_j}\left(\rho \overline{u_i u_j}\right) = \frac{\partial \rho}{\partial x_i} + \frac{\partial}{\partial x_j}\left[\eta\left(\frac{\partial \overline{u}_i}{\partial x_j} + \frac{\partial \overline{u}_j}{\partial x_i}\right) - \rho \overline{u_i' u_j'}\right] + g_j(\rho - \rho_0), \tag{2}$$

$$\frac{\partial(\rho\bar{c})}{\partial t} + \frac{\partial}{\partial x_j}\left(\Gamma\frac{\partial c}{\partial x_j}\right) - \frac{\partial}{\partial x_j}\left(\rho\overline{u_j'c'}\right), \quad (3)$$

where ρ is the density field, c the concentration scalar field, η the dynamic viscosity, and Γ the diffusivity. Due to the Reynolds decomposition, it is crucial to model the cross correlations of the velocity fluctuations $\overline{u_i'u_j'}$ (known as the Reynolds and shear stresses) as well as the turbulent fluxes $\overline{u_j'c'}$. According to Petrov and Manera [16], currently available models for turbulent momentum fluxes will more likely lead to an overestimation for thermal stratification but an underestimation for turbulent mixing when buoyancy effects dominate the mass transportation in the flow. Thanks to the local isotropy assumptions used in most subgrid-scale models, even LESs cannot adequately capture for the behavior of a buoyant jet in the presence of thermal stratification. To gain more physical insight and improve existing CFD models for buoyancy driven flows in the presence of stratification, it is pivotal to experimentally construct a high-resolution high-fidelity database.

Nonintrusive optical measurement techniques like particle image velocimetry (PIV) and planar laser-induced fluorescence (PLIF) can get velocity and concentration fields with high spatial and temporal resolutions.

However, a phenomenon called Schlieren caused by optical inhomogeneities (different refractive indices) in transparent materials will lead to blurred images, making the application of optical measurement techniques resulting in biased and erroneous measurements of velocity and concentration fields. To prevent the laser sheet which is used to illuminate the flow and the light scattered by the tracing particles from getting deflected due to the changes of densities, it is essential to match the refractive indices for the solutions used in the experiments. For this purpose, a novel Refractive Index Matching (RIM) technique was developed and demonstrated by Krohn et. al [17]. This technique eliminates the issues associated with the laser light diffraction and image distortion. Qin et al. [18] presented high resolution velocity measurements of turbulent round jets, obtained with high-speed Particle Image Velocimentry (PIV). They focused on the near-field and the self-similar regions of the jet, analysing the entrainment and momentum transport. Using the novel RIM technique applied to PIV and Laser Induced Fluorescence (LIF)measurements, Qin et al. [19] analyzed the turbulent statistics in the self-similar region of positive and negative buoyant jets, in the presence of a 3.16% density difference. Qin et al. in reference [20] studied turbulent buoyant jets and their interaction with a two-layer stratified environment based on high-resolution velocity and concentration data.

The goal of the present study is to investigate the effect of buoyancy and of a two-layer stratified environment on turbulent buoyant jets based on planar PIV and LIF measurements. The study includes both cases with a two-layers stratified environment and cases with uniform environment for comparison (see Figure 1). The experiments considered are summarized in Table 1. Cases with different level of turbulence, expressed by the Reynolds number, and of buoyancy with respect to shear, expressed by the Richardson number were investigated, both in uniform and stratified environment.

The Reynolds number along the jet's axis is defined as:

$$\mathrm{Re}(x_0, y) = \frac{DV(x_0,y)}{\nu(x_0,y)}, \quad (4)$$

where D is the diameter of the jet's orifice, $V(x_0, y)$ is the time-averaged vertical velocity on the axis of the jet ($x = x_0, y$). and υ is the kinematic viscosity of the fluid.

The Richardson number is expressed as:

$$\mathrm{Ri} = gD\frac{\rho_{env.}-\rho_{jet}}{\rho_{jet}V_0^2}, \quad (5)$$

where g is the magnitude of the vertical acceleration, $\rho_{env.}$ is the mass density of the environment where the jet is injected, ρ_{jet} is the mass density of the jet at the orifice, and V_0 is the jet's velocity at the orifice. Mean velocity and concentration profiles, turbulent Reynolds stresses, turbulent concentration fluxes and entrainment are presented.

1.1. Methods

The jet's development, turbulent Reynolds stresses, concentration fluxes and entrainment, are experimentally studied in (buoyant) jets with uniform and stratified environments. The effect of buoyancy is studied by mixing fluids with different densities and the same refractive index.
The novel Refractive Index Matching (RIM) method [17], which was developed at the Experimental and Computational Multiphase Flow Laboratory of the University of Michigan, allows us to measure with high accuracy the mixing of fluids up to a density difference of 8.6% extending the capabilities of available RIM methods. The novel method is based on the behavior of excess properties and their change in a multicomponent system while mixing. With this technique, one can study buoyancy without heating the fluid. When a large density difference (e.g., above 5-10%) is obtained by heating a fluid, the results of the measurements are affected by non-Oberbeck-Boussinesq effects [22, 23, 24], because the approximation of constant fluid properties and density that depends linearly on temperature only in the buoyancy term is not applicable. The mixing of fluids with non-uniform refractive index causes deviations of the laser light and of the light scattered by the seeding particles [25, 26, 27]. Both effects challenge PIV and LIF experiments. With the RIM method, one can use optical techniques like PIV and LIF with high accuracy. In the present study LIF measurements are used together with PIV simultaneously, to study the mixing of buoyant jets with the environment. The jet's fluid is marked with a tracer compound, while the environment contains fresh fluid. In the experiments with 3.16% density difference, a combination of two aqueous solutions with sodium sulfate (Na_2SO_4) and glycerol (H_2O – $CH_2OHCHOHCH_2OH$) is used. In the measurements with 8.6% density difference, the liquids used are ternary solutions of water, isopropanol ($CH_3CHOHCH_3$), and glycerol. All three liquids are fully miscible among each other, and the two solutions exhibit a large density difference. Velocity and concentration measurements are performed in the self-similar region of the jet. The raw data used in this work were published in the Ph.D. thesis of S. Qin [21].

1.2. Experimental Set-up

The experimental set-up and instrumentation are described in detail in reference [21], we report here a summary of the most important characteristics. The miniDESTROJER (DEnsity Stratified Turbulent ROund free Jet ExpeRiment) facility at the University of Michigan is a facility designed to study turbulent buoyant jets in stratified environments using optical measurements. It is composed of a tank with glass walls with an orifice of 2 mm diameter at the bottom. The tank size is 300 mm × 300 mm × 300 mm. The corresponding tank size-to-nozzle ratio is 150, ensuring the flow is an unconfined free jet. The axial jet flow is driven with a piston powered by a Dynamic Motor Motion Servo engine that ensures a precise and controllable inlet velocity profile. A scheme of the miniDESTROJER test section for experiments with uniform and stratified environment is shown in Figure 1.
Planar PIV is used to measure instantaneous velocity fields on a vertical section of the jet in the self-similar region, at a downstream location from 40 to 80 orifice diameters. The RIM method was applied to measure buoyant jets with density differences up to 8.6%. The instrumentation for the PIV measurements consists of one high-speed laser with optics, one high-speed camera, a synchronizer, and a software for data acquisition and processing. The highspeed double pulsed laser is a Nd:YLF laser from Photonics Industries International Inc. with a maximum pulse frequency of 10 kHz at a wavelength of 527 nm and 70 mJ energy per pulse. It is equipped with two spherical and one cylindrical lens, with focal length $f = 10$mm, to create a laser sheet. The camera is a Phantom Miro LAB M340 highspeed CMOS with 2,560 × 1,600 pixels, pixel size of 10 μm, and 800 Hz maximum frame rate at full resolution. The seeding particles are hollow glass spheres with diameter of 10 μm and mass density of 1,10±0,05 g/cm^3. The software DaVis 8.4 from LaVision® GmbH was used for data acquisition and processing. The processing of the PIV data is described in [21].

For the LIF measurements, Rhodamine-6G is used as tracer to characterize the scalar field of the jet flow. The laser light at a wavelength of 532 nm, acts on the tracer molecules exciting and causing the same to emit fluorescent signals. Images are captured by a CMOS digital camera equipped with a light filter permeable to the particle's emission wavelength of 570 nm. The PIV and LIF measurements are synchronized to have simultaneous velocity and concentration fields on the same vertical section of the jet.

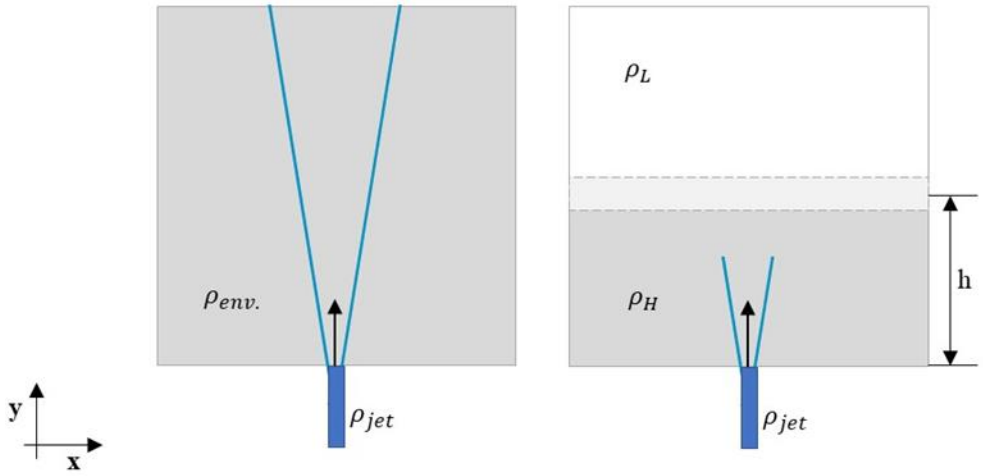

Figure 1: Scheme of the experiments of jets with uniform (left) or stratified environment (right). ρ_{jet} and $\rho_{env.}$ are the densities of the jet and the environment fluid, respectively. ρ_H and ρ_L are the densities of the heavy and the light fluid, respectively. h is the vertical distance from the jet orifice. x and y are the horizontal and vertical axis, respectively.

1.3. Experimental Programme

The experimental test matrix includes cases of turbulent buoyant jets in uniform and stratified environment, and reference cases of jets in uniform environment. Table 1 reports the experimental conditions of all cases studied, the jet's velocity at the orifice (V_0), the mass density of the jet and the one of the environment (ρ_{jet} and ρ_{env}, respectively), the temperature of the set-up (T), the Reynolds and Richardson numbers of the jet, defined as in equations (4) and (5), respectively. The cases investigated can be grouped in four categories:

- Positive buoyant jets in uniform environment, when the density of the jet is lighter than the density of the environment ($\rho_{jet} < \rho_{env}$). Cases D033 and D034 are characterized by a relative density difference between the environment and the jet of 3.16 % $\left(\frac{\rho_{jet}-\rho_{env.}}{\rho_{jet}} = 3.16\%\right)$, while cases D051 and D052 by a relative density difference of 8.6%.
- Negative buoyant jets in uniform environment, when the density of the jet is heavier than the density of the environment ($\rho_{jet} > \rho_{env}$). Cases D035 and D036 are negative buoyant jets with a negative density difference of 3.16%, while cases D047 and D048 have a negative density difference of 8.6%.
- Positive buoyant jets in stratified environment. Cases D042 and D043 have a density difference with respect to the environment (bottom layer) of 3.16%. As shown in Figure 1, right side, the environment is stratified, at the bottom there is heavy fluid with density equal to the one of the jet, and at the top (above the height of h) there is air.
- Jets in uniform environment. These cases are used as a reference of no buoyancy. They are case D029 ÷ D032, D045, D049, D049, and D050.

Table 1: Summary of experiments in uniform environment without buoyancy (D029 ÷ D032, D045, D046, D049, D050), in uniform and stratified environment with relative density difference ($\Delta\rho$) of 3.16% (D033 ÷ D036, D042 and D043), and in uniform environment with $\Delta\rho$ of 8.6% (D047, D048, D051, and D052). V_0 is the jet's velocity at the orifice. ρ_{jet} and ρ_{env} are the mass density of the jet and the environment, respectively. T is the temperature of the set-up. Re and Ri are the Reynolds and Richardson's numbers of the flow, defined in eq. (4) and (5), respectively.

Case	[m/s]	ρ_{jet} [kg/m^3]	ρ_{env} [kg/m^3]	$\Delta\rho$ [%]	T [°C]	Re	Ri [×10^{-5}]
D029	5.990 ± 0.004	1012.0 ± 10.1		0	20.4 ± 0.1	10000	
D030	2.460 ± 0.002	1012.0 ± 10.1		0	20.4 ± 0.1	4000	
D031	5.530 ± 0.004	1044.0 ± 10.4		0	20.0 ± 0.1	10000	
D032	2.300 ± 0.002	1044.0 ± 10.4		0	20.0 ± 0.1	4000	
D045	9.060 ± 0.006	1011.0 ± 10.1		0	19.2 ± 0.1	4000	
D046	4.220 ± 0.003	1011.0 ± 10.1		0	19.3 ± 0.1	2000	
D049	9.060 ± 0.006	924.3 ± 9.2		0	18.4 ± 0.1	4000	
D050	4.220 ± 0.003	924.3 ± 9.2		0	18.6 ± 0.1	2000	
D033	5.990 ± 0.004	1012.0 ± 10.1	1044.0 ± 10.4	3.16	20.4 ± 0.1	10000	1.73
D034	2.460 ± 0.002	1012.0 ± 10.1	1044.0 ± 10.4	3.16	20.4 ± 0.1	4000	10.3
D035	5.530 ± 0.004	1044.0 ± 10.4	1012.0 ± 10.1	3.16	20.0 ± 0.1	10000	-1.97
D036	2.300 ± 0.002	1044.0 ± 10.4	1012.0 ± 10.1	3.16	20.5 ± 0.1	4000	-11.4
D042	5.990 ± 0.004	1012.0 ± 10.1	Stratification		18.1 ± 0.1	10000	
D043	2.460 ± 0.002	1012.0 ± 10.1	Stratification		19.0 ± 0.1	4000	
D047	9.060 ± 0.006	1011.0 ± 10.1	924.3 ± 9.2	8.60	19.3 ± 0.1	4000	-2.05
D048	4.220 ± 0.003	1011.0 ± 10.1	924.3 ± 9.2	8.60	19.7 ± 0.1	2000	-9.45
D051	9.060 ± 0.006	924.3 ± 9.2	1011.0 ± 10.1	8.60	18.5 ± 0.1	4000	+2.00
D052	4.220 ± 0.003	924.3 ± 9.2	1011.0 ± 10.1	8.60	18.8 ± 0.1	2000	+10.3

2. RESULTS

Vertical mean velocity profiles at the axis location ($y/D = 40$) normalized by the initial velocity (V_0) for all the experiments considered (see Table 1) are shown in Figure 2 with errorbars according to the uncertainty estimation of Qin [21]. We can observe a collapse of the radial velocity profile for all the experiments without influence of Reynolds and Richardson numbers. This confirms the results of Hrycak et al. [28], which showed that for an axisymmetric jet, the radial velocity profile when normalized by the centerline velocity, is mostly independent of the Reynolds number in the turbulent flow region.
The Full Width at Half Height (FWHH) of the vertical velocity profile has the same slope for all experiments, except for case D043 (Figure 3). This experiment, together with case D042, is characterized by a two-layer stratified environment with a sharp interface (see **Table 1**). It has a lower Reynolds number than case D042 (Re $= 4000$, instead than Re $= 10000$) and therefore less momentum force. This is the reason why the jet's width after the interface, at approximately $\frac{y}{D} = 60$, starts to deviate from the one of the other experiments. The mean velocity on the jet's axis normalized by the velocity at the orifice (V_m/V_0) has a similar slope for all experiments, except for case D043 (Figure 4). The speed of this jet starts to decrease drastically at about $\frac{y}{D} = 70$. The slope of V_m/V_0 as a function of distance from the jet's orifice along the axis is, for the cases without stratification and for the one with stratification and large Reynolds number, in good agreement with the reference value reported in the literature from previous experiments in turbulent jets [7]. The results of Figure 3 and Figure 4 are explained by the fact that in the experiments with a stratified environment, when Re = 10000, as in case D042, the turbulent jet has

enough momentum to penetrate through the top fluid surface. However, when the Reynolds number decreases as in case D043, the jet interacting with the density interface behaves like a fountain: it reaches a final maximum height, and then falls back to the density interface, interacting with the layer and the upcoming flow.

The inverse of the mean tracer concentration on the jet's axis multiplied by the concentration at the orifice (C_0/C_m) shows a similar slope for all jets with or without buoyancy, except for the two cases with stratified environment (Figure 5). For these two cases, we observe an increase of concentration starting below the location of the interface. The slope of the experiments in uniform environment agrees quite well with the one from past studies from the literature [7].

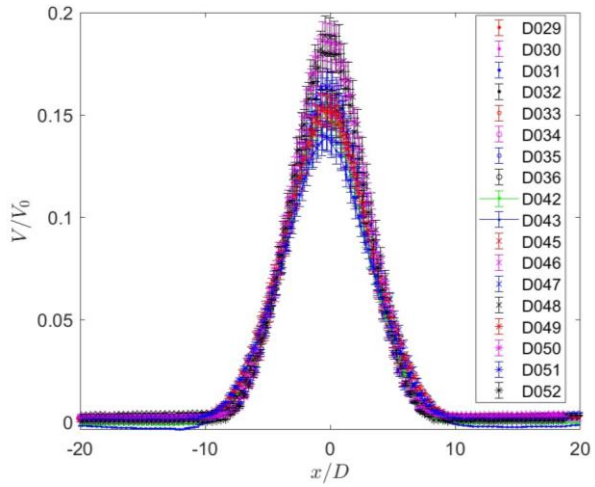

Figure 2: Spanwise velocity at $\frac{y}{D} = 40$, with errorbars.

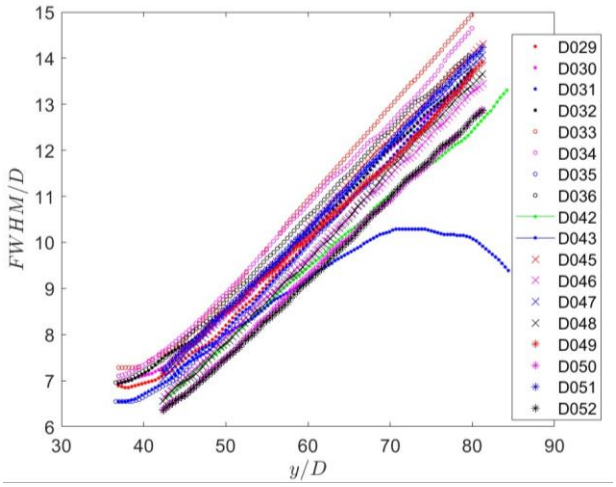

Figure 3: Full Width at Half Maximum (FWHM) of the mean velocity profile.

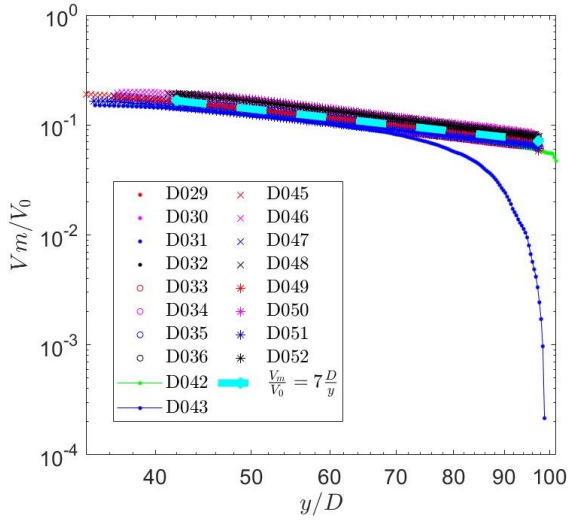

Figure 4: Mean velocity on the axis of a turbulent jet as a function of distance from the jet orifice.

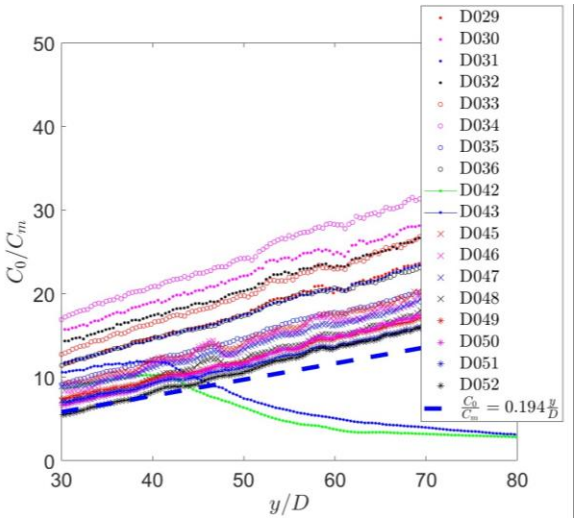

Figure 5: Mean concentration on the axis of a turbulent jet as a function of distance from the orifice.

The evolution of the Reynolds number along the jet's axis for positive and negative buoyant jets with different speeds at the orifice is shown in Figure 6. The local Reynolds number and the Richardson number are computed as in equations (4) and (5), respectively. The kinematic viscosity used to compute

the local Reynolds number is a function of the tracer concentration measured from the LIF experiments [19]. From Figure 6 we can observe that the Reynolds number along the jet's axis depends on the value of the Reynolds and Richardson numbers at the orifice. Indeed, cases D033 and D035 that are characterized by a larger initial Reynolds number (Re = 10000), have larger Reynolds along the axis with respect to cases D034 and D036 (Re = 4000). Cases D033 and D034 that have a positive initial Richardson number (Ri_0) show larger values of Reynolds along the axis with respect to cases D035 and D036, respectively, at equal initial Reynolds number. This confirms what was observed by Nathan [29] that only the jet inlet conditions will influence both the near-field and downstream flows, because they contribute to the structures of the turbulent motions that are carried from the jet nozzle throughout the flow. Figure 7 shows the data of Figure 6 normalized by the Reynolds number at the orifice (Re_0). We can observe that after normalization the values of Reynolds along the axis are ordered according to Ri, which means that buoyancy has a positive effect on the jet's speed. Figure 8 shows in addition four experiments of pure jets in uniform environment without buoyancy (case D029, D030, D031, and D032, see **Table 1** for details). We can see that these experiments are located approximately between the cases with positive and the ones with negative Richardson number. If we consider the experimental cases with 8.6% density difference, see Figure 9, we cannot observe that the values of the Reynolds number along the axis are ordered according to Ri. This may be due to uncertainties in the measurements of the kinematic viscosities of the two solutions used, due to the high volatility of isopropanol.

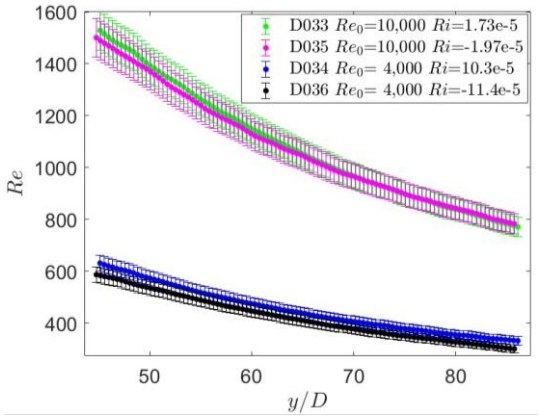

Figure 6: Reynolds number at the jet's centerline for experiments D033, D034, D035, and D036.

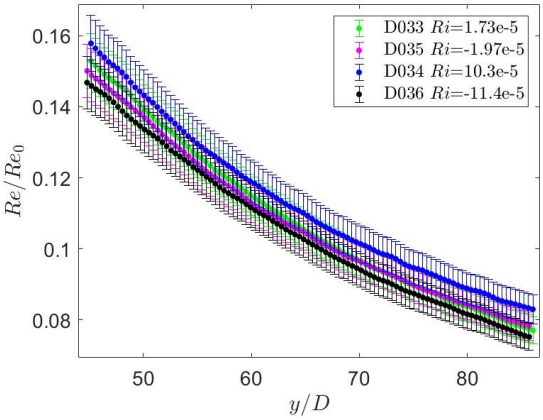

Figure 7: Reynolds number at the jet's centerline normalized by the Reynolds number at the orifice, for experiments D033, D034, D035, and D036.

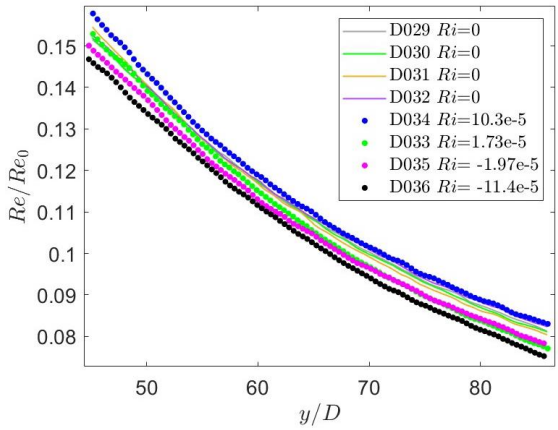

Figure 8: Reynolds number at the jet's centerline normalized by the Reynolds number at the orifice, for experiments D029, D030, D031, D032, D033, D034, D035, and D036.

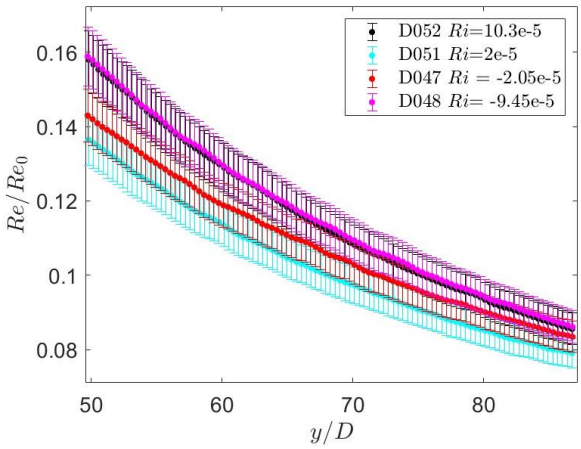

Figure 9: Reynolds number calculated at the jet's centerline normalized by the Reynolds number at the orifice, for experiments D047, D048, D051, and D052.

The Probability Density Function (PDF) of the mass density of cases D033, D034, D035, and D036 at two locations along the jet's axis is shown in Figure 10 and Figure 11. One can see that the density at fixed y/D exhibits one peak and a plateau towards smaller values. The peak represents the density of the injected fluid, while the plateau the mixing region with the environment. For all cases, the width of the PDF at $\frac{y}{D} = 80$ is smaller than at $\frac{y}{D} = 40$. This is an indication of better mixing further away from the jet's orifice. Also, the maximum peak at $\frac{y}{D} = 80$ is slightly smaller, indicating that the jet is better mixed with the environment. Cases D033 and D034 (Figure 10) are characterized by a positive density difference between the jet and the environment (positive buoyant jets), while cases D035 and D036 (Figure 11) by a negative one. Comparing Figure 10 and Figure 11, we can see that the width of the PDFs is smaller for positive buoyant jets. This is an indication that buoyancy enhances mixing. Also, the width of the PDFs is larger for case D033 than for case D034 (Figure 10), and for cases D035 than for D036 (Figure 11). Indeed, cases D034 and D036 have a smaller Reynolds number than cases D033 and D035, and a larger magnitude of the Richardson number, indicating that a larger effect of buoyancy with respect to shear helps mixing.

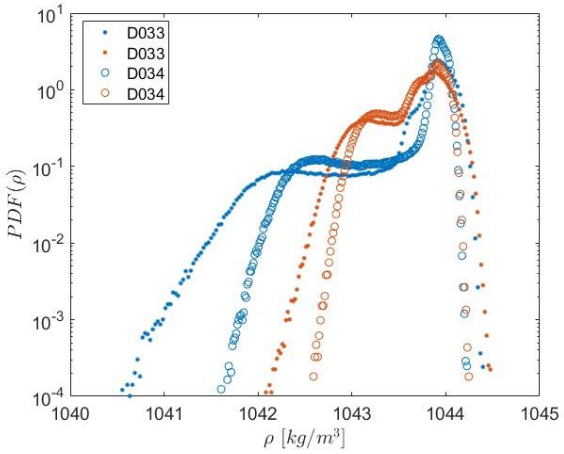

Figure 10: Probability Density Function (PDF) of the mass density of cases D033 and D034 at two locations along the jet's axis $\frac{y}{D} = 40$ (blue), and $\frac{y}{D} = 80$ (red).

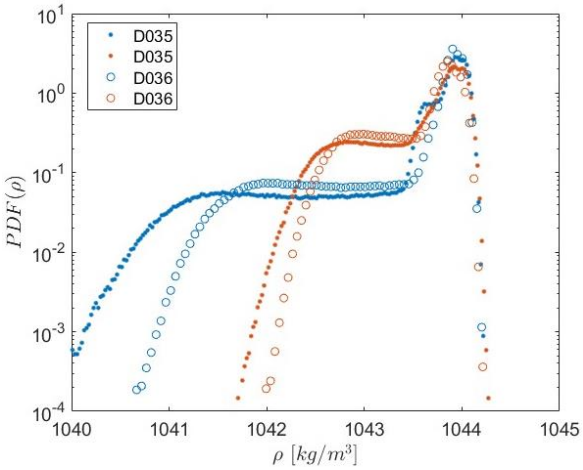

Figure 11: Probability Density Function (PDF) of the mass density of case D034 at two locations along the jet's axis $\frac{y}{D} = 40$ (blue), and $\frac{y}{D} = 80$ (red).

The turbulent shear stress is defined as: $\tau(x,y) = \frac{\overline{u'(x,y,t)\cdot v'(x,y,t)}}{V^2(x_0,y)}$, where $\overline{u'(x,y,t)\cdot v'(x,y,t)}$ is the time average of the fluctuating velocity components u' (horizontal) and v' (vertical). (x,y,t) are the horizontal, vertical, and time coordinates as shown in Figure 1, and $V(x_0,y)$ is the vertical velocity along the axis of the jet ($x = x_0$). Figure 12 shows the turbulent shear stress at the position of $\frac{y}{D} = 60$, for all the experiments and two references from the literature (Wygnanski [30] and Rodi [31]). We can see that all experimental cases and the two literature references well agree with each other, and the only exception is case D043, the one with stratified environment and lower Reynolds number.
Analogously to the turbulent shear stress, the turbulent concentration fluxes in the vertical and horizontal direction, τ_{vc} and τ_{uc} respectively, are defined as: $\tau_{vc} = \frac{\overline{v'(x,y,t)\cdot c'(x,y,t)}}{V(x_0,y)\cdot C(x_0,y)}$ and $\tau_{uc} = \frac{\overline{u'(x,y,t)\cdot c'(x,y,t)}}{U(x_0,y)\cdot C(x_0,y)}$, where $C(x_0,y)$ is the vertical concentration and $U(x_0,y)$ the horizontal velocity along the axis.

Figure 13 and Figure 14 show the turbulent concentration fluxes τ_{vc} and τ_{uc}, respectively, at the axial position of $\frac{y}{D} = 60$. τ_{vc} and τ_{uc} are plotted as a function of the horizontal dimension $x/r_{1/2}$, where $r_{1/2}$ is the lateral dimension where the jet's vertical velocity is equal to the half of its maximum value. From Figure 13 and Figure 14, one can observe that no differences emerge among the experimental cases considered, except for the two jets with stratified environment (D042 and D043). For these two experiments we note that the turbulent concentration fluxes have a smaller magnitude in the central part of the jet and a wider distribution in the horizontal direction (x). This is an indication that the sharp stratification in the environment induces the jet to spread horizontally at the level of the interface.

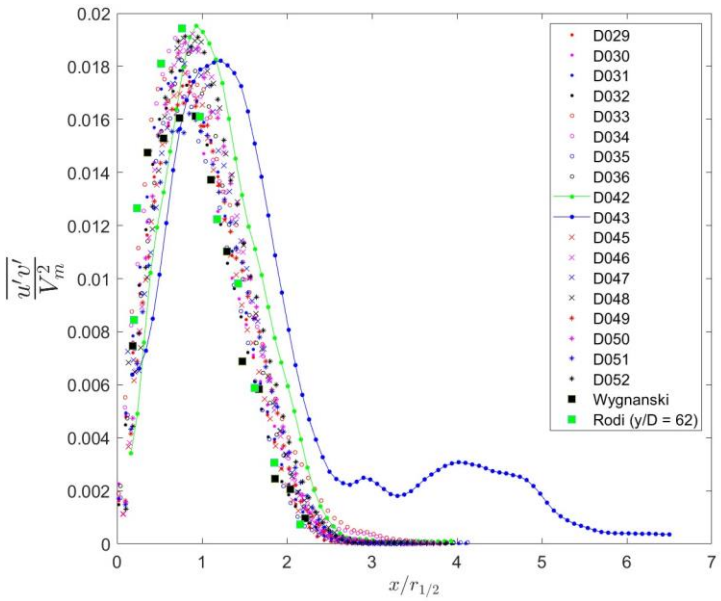

Figure 12: Turbulent shear stress at y/D = 60.

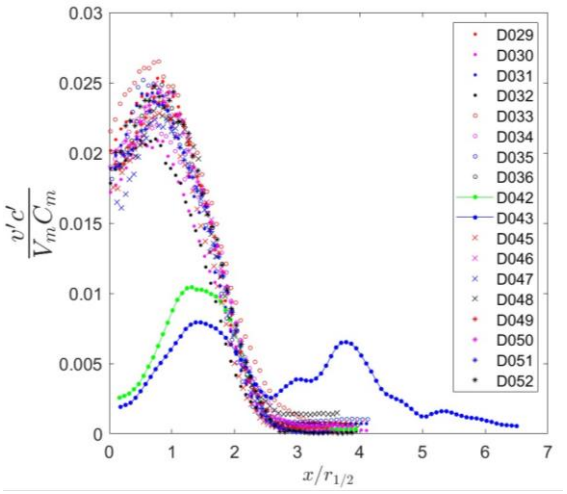

Figure 13: Turbulent concentration flux at y/D = 60.

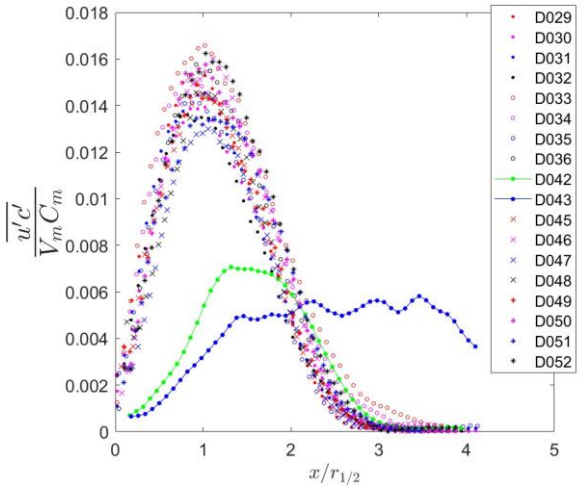

Figure 14: Horizontal turbulent concentration flux at y/D = 60.

Figure 15 shows the volume flux as a function of distance from the jet origin for all experimental cases. The volume flux is defined as the ratio between the entrainment (μ) and the jet specific mass flux at the orifice ($Q = \rho_0 V_0 A$, where ρ_0 is the mass density and V_0 the jet's velocity at the orifice, while A is the cross-section). The entrainment is defined as: $\mu(y) = \int_0^{L(x)} V(x,y) 2\pi x \, dx$, where V is the time-averaged vertical velocity, and L is the characteristic length of the jet. From Figure 15 one can observe that the volume flux is the lowest for the two jets injected in sharp environment, D042 and D043. For case D042, which has lower Reynolds number, the volume flux drastically decreases in correspondence with the position of the interface (about $\frac{y}{D} \simeq 60$). One can also see that the cases with the largest Richardson numbers D034 and D052 have lower values of entrainment with respect to the other cases with uniform environment. The case with the largest volume flux is D048, which is characterized by a large negative

Richardson number. From this comparison, one can conclude that a stratified environment and the Richardson number have a large influence on the volume flux and its evolution along the jet's axis. A stratified environment and a large positive Richardson number are responsible for low values of volume flux. The same plot presents a reference slope from the experimental literature review of List [7] for comparison.

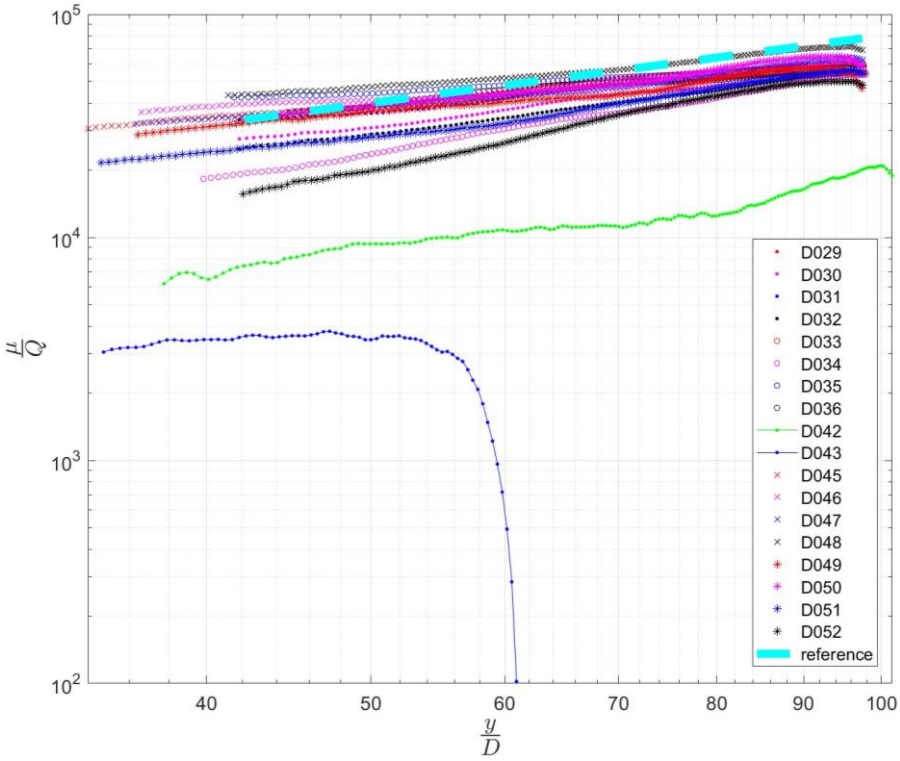

Figure 15: Volume flux as a function of distance from the jet origin for all experimental cases. Reference line from [7].

3. CONCLUSIONS

In this study, we analyze positive, negative, and neutral buoyant jets, both in a uniform and in a two-layer stratified environment. The investigation is based on simultaneous PIV and LIF measurements in the self-similar region of the jet. A novel RIM method is applied to perform accurate measurements with density differences up to 8.6%, while matching the refractive index of the mixed solutions. We observe that the two cases with a stratified environment show significant differences with respect to the other ones. The case in stratified environment and lower Reynolds number is characterized by a full width at half height that decreases after the sharp interface in the stratified environment, while the same quantity increases linearly for all other cases. For this experiment, also the maximum velocity decreases after the interface, while it increases for the other ones. The concentration on the jet's axis for both cases in stratified environment increases starting from below the heigh of the stratification interface in the environment. The turbulent shear stress and the concentration fluxes show that the case in stratified environment with lower Reynolds number spreads horizontally at approximately the height of the interface, behaving like a fountain. Instead, no significant differences are visible among the experiments in uniform environment. Only the value of the Reynolds number along the jet's axis is slightly larger for larger inlet Richardson numbers in the experiments with density differences of 3.16%. This trend is not visible in the cases with 8.6% density difference. The reason might be related to a larger uncertainty in the value of the kinematic viscosity of the latter experiments, due to the high volatility of one component of the solutions used.

This study can be extended in several directions. One regards the investigation of the effect of a linearly stratified environment on the buoyant jets. This is a closer representation than a two-layer environment to what occurs in real applications, like for example in the upper plenum of the hot pool of sodium-cooled fast reactors. A further direction consists in pushing the current limit of 8.6% density difference of the RIM method, by finding new possible combinations of aqueous solutions. The results of this study on buoyant jets in stratified environment will be used for the validation of commercial CFD codes.

Bibliography

[1] D. Paladino, M. Andreani, R. Zboray and J. Dreier, "Toward a CFD-grade database addressing LWR containment phenomena," *Nuclear Engineering and Design,* vol. 253, pp. 331-342, 2012.

[2] E. Deri, B. Cariteau and D. Abdo, "Air fountains in the erosion of gaseous stratifications," *International Journal of Heat and Fluid Flow,* vol. 31, pp. 935-941, 2010.

[3] F. E. Dunn, T. H. Fanning and J. E. Cahalan, "Preliminary safety evaluation of the advanced burner test reactor.," United States, 2006.

[4] G. Abraham, Jet diffusionin stagnant ambient fluid, Delft University of Technology: Doctoral Thesis, 1963.

[5] J. Turner, "Jets and plumes with negative or reversing buoyancy," *Journal of Fluid Mechanics,* vol. 26, pp. 779-792, 1966.

[6] H. Fischer, E. List, C. Koh, J. Imberger and N. Brooks, Mixing in Inland and Coastal Waters, Academic Press, 1979.

[7] E. J. List, "Mechanics of Turbulent Buoyant Jets and Plumes," in *HMT: the Science & Applications of Heat and Mass Transfer. Reports, Reviews & Computer Programs*, Pergamon, 1982, pp. 1-68.

[8] L. Bloomfield and R. Kerr, "Turbulent fountains in a stratified fluid," *Journal of Fluid Mechanics,* vol. 358, pp. 335-356, 1998.

[9] L. Bloomfield and R. Kerr, "A theoretical model of a turbulent fountain," *Journal of Fluid Mechanics,* vol. 424, pp. 197-216, 2000.

[10] Y. Lin and P. Linden, "The entrainment due to a turbulent fountain at a density interface," *Journal of Fluid Mechanics,* vol. 542, pp. 25-52, 2005.

[11] R. Mott and A. Woods, "On the mixing of a confined stratified fluid by a turbulent bouyant plume," *Journal of Fluid Mechanics,* vol. 623, pp. 149-165, 2009.

[12] S. Shy, "Mixing Dynamics of Jet Interaction with a Sharp Density Interface," *Experimental Thermal and Fluid Science,* vol. 10, pp. 355-369, 1995.

[13] P. J. Ansong, J. K. Kyba and B. Sutherland, "Fountains impinging on a density interface," *Journal of Fluid Mechanics,* vol. 595, pp. 115-139, 2008.

[14] S. Shakouchi, S. Fukue and T. Uchiyama, "Investigation of the Behavior of a Jet Issued into Two-Layer Density-Stratified fluid," *Journal of Flow Control, Measurement & Visualization,* 2014.

[15] H. Fernando, "Turbulent mixing in stratified fluids," *Annual Reviews of Fluid Mechanics,* vol. 23, pp. 155-93, 1991.

[16] V. Petrov and A. Manera, "Validation of STAR-CCM+ for buoyancy driven mixing in a PWR reactor pressure vessel," in *Proceedings of 14th Int. Topical Meeting on Nuclear Reactor Thermal-hydraulics (NURETH-14)*, Toronto, Canada, 2011.

[17] B. Krohn, A. Manera and V. Petrov, "A novel method to create high density stratification with matching refractive index for optical flow investigations," *Experiments in Fluids,* p. 59:66, 2018.

[18] S. Qin, B. Krohn, J. Downing, V. Petrov and A. Manera, "High-Resolution Velocity Field Measurements of Turbulent Round Free Jets in Uniform Environments," *Nuclear Technology,* 2018.

[19] S. Qin, B. Krohn, V. Petrov and A. Manera, "Velocity and Scalar Fields of a Turbulent Buoyant Jet in the Self-Similar Region," *Nuclear Technology,* pp. 307-321, 2019.

[20] S. Qin, V. Petrov and A. Manera, "Velocity - and scalar - field measurements of turbulent bouyant round jets in a two-layer stratified envronment," in *Proceedings of 18th Int. Topical Meeting on Nuclear Reactor Thermal-hydraulics (NURETH-18)*, Portland, Oregon, United States, 2019.

[21] S. Qin, High-Resolution Experiments and Computations on Mixing of Turbulent Buoyant Round Free Jets in Uniform and Stratified Environments, University of Michigan, 2020.

[22] V. Valori, G. E. Elsinga, M. Rohde, M. J. Tummers, J. Westerweel and T. H. J. J. van Der Hagen, "Natural convection driven heat transfer in fluids with strongly variable properties: A particle image velocimetry study," in *16th International Topical Meeting on Nuclear Reactor Thermal Hydraulics*, Chicago, Illinois, United States, August 30-September 4, 2015.

[23] V. Valori, G. E. Elsinga, M. Rohde, M. Tummers, J. Westerweel and T. H. J. J. van der Hagen, "Experimental velocity study of non-Boussinesq Rayleigh-Bénard convection," *Physical Review E,* vol. 95, no. 5, p. 053113, 2017.

[24] H. Yik, V. Valori and S. Weiss, "Turbulent Rayleigh-Bénard convection under strong non-Oberbeck-Boussinesq conditions," *Physical Review Fluids,* vol. 5, no. 10, p. 103502, 2020.

[25] V. Valori, G. E. Elsinga, M. Rohde, J. Westerweel and T. H. J. J. van der Hagen, "Particle image velocimetry measurements of a thermally convective supercritical fluid," *Experiments in Fluids,* vol. 60, p. 143, 2019.

[26] G. Elsinga, B. van Oudheusden and F. Scarano, "Evaluation of aero-optical distortion effects in PIV," *Experiments in Fluids,* vol. 39, pp. 246-256, 2005.

[27] V. Valori, Rayleigh-Bénard convection of a supercritical fluid: PIV and heat transfer study, Doctoral Thesis, Delft University of Technology, 2018.

[28] P. Hrycak, S. Jachna and D. Lee, "A study of characteristics of developing, incompressible, axi-symmetric jets," *Letters in Heat and Mass Transfer,* vol. 1, pp. 63-72, 1974.

[29] G. J. Nathan, J. Mi, Z. T. Alwahabi, G. J. R. Newbold and D. S. Nobes, "Impacts of a jet's exit flow pattern on mixing and combustion performance," *Progress in Energy and Combustion Science,* vol. 32, pp. 496-538, 2006.

[30] I. Wygnanski and H. Fiedler, "Some measurements in the self-preserving jet," *Journal of Fluid Mechanics*, vol. 38, pp. 577-612, 1969.

[31] W. Rodi, "A new method of analysing hot-wires signals in highly turbulent flow, and its evaluation in a round jet," in *DISA Info*, 1975.